A Configurable IC to Contol, Readout, and Calibrate an Array of Biosensors

Sara S. Ghoreishizadeh, Sandro Carrara, and Giovanni De Micheli
EPFL, LSI - Lausanne - Switzerland

***Abstract*—We present a novel integrated circuit for a biosensing data acquisition chain. The circuit controls and reads out five bimolecular sensors as well as pH and temperature sensors for biosensor calibration. The IC supports both *chronoamperometry* (CA) and *cyclic voltammetry* (CV) measurements, which are commonly used in biosensing. Different voltage waveforms are generated to control CV by using a single configurable waveform generator and programmable constant voltage levels are produced to enable CA. To reduce the area and power consumption of the interface electronics, a unified circuit is designed for CV, CA and pH readout. The biosensors produce currents that are converted by a 13.5-bit sigma delta analog to digital converter. The circuit has been designed and realized in $0.18\ \mu m$ technology. It consumes $711\ \mu W$ from a $1.8\ V$ supply voltage, making it suitable for remotely powered and implantable applications.**

***Index Terms*—Interface electronics; Multi-target biosensor; CV and CA readout; Temperature and pH readout; CMOS IC.**

I. Introduction

Biosensors are used to monitor patients in critical and/or chronic conditions, where often the concentration of molecules, typically metabolites, is important. Endogenous molecules (e.g., glucose, lactate, ATP) and exogenous molecules (e.g., etoposide and ifosfamide for chemotherapy) often need for monitoring. Some biosensors are designed to be worn or implanted, thus requiring minimal volume.

Biosensors consist of transducers and an electronic control/readout circuit. The electrochemical transducers implement miniaturized electrochemical cells, abstracted by three-terminal devices. Electrodes are usually called *working electrode* (WE), *reference electrode* (RE), and *counter electrode* (CE). The most common operation modes are *chronoamperometry* (CA) and *cyclic voltammetry* (CV) [1]. CA is typically used for detecting endogenous molecules with oxidases, while CV is required for detecting exogenous compounds with cytochromes [2], [3]. CA and CV measure a current out of a terminal (WE or CE) when a fixed or variable voltage is applied to the other two, respectively. Many works have been done to integrate the CA readout electronics for implantable three electrode based biosensors [4-6]. In [7] a CV readout IC with 9-bit resolution is presented. In [8] a CA and CV control and readout IC is presented which consumes more than $20\ mW$. This paper describes a new high resolution (13.5-bit) and low power ($711\ \mu W$) control and readout IC in $0.18\ \mu m$ technology to support both CA and CV for an array or 5 molecular transducers.

The calibration of the biosensors with environmental variables like pH and temperature is required for precise monitoring [9]. However, this has not been addressed yet in the current state of the art integrated interface electronics. We also present new circuits for pH and temperature readout for calibration. To enable miniaturization of the biosensor, the array of the transducers uses a common RE and CE.

This circuit is -to the best of our knowledge- the first complete and integrated realization to support multiple molecular measurements based on enzymes like oxidases and cytochromes, as well as sensor calibration. It address several challenges, including, but not limited to, low-power, low-noise, high accuracy realization, slow electrostatic control (to match molecular dynamics), and small current sensing.

In particular, for CV, it is important to generate a high amplitude sub-Hertz triangular waveform to control the transducer. In this work a *direct digital synthesizer* (DDS) is used to generate sub-Hertz triangular waveforms [10].

Moreover, the circuit has to drive multiple transducers with different *resistor-capacitor* (RC) equivalent models, that may be time and concentration dependent. Since the transducer is the load of the readout circuit, its variation can drive the circuit into instability. To address this, a highly stable readout circuit for wide range of load capacitances has been designed.

Almost all biosensors need considerable time (upto an hour) for conditioning before being prepared for a measurement. To realize fast and real time monitoring of different molecules, parallel conditioning and measurement for different sensors is made possible in this IC using a configurable interface circuit.

In the following section, different parts of the system are described. Simulation results are presented in Section III followed by the conclusion.

II. System Design

The simplified schematic view of the configurable control and readout IC for the multi-target biosensor is shown in Fig. 1. It consists of a unified measurement block for CV, CA and pH readout followed by a sigma-delta *analog to digital converter* (ADC). To speed up the measurements, two conditioning circuits are also designed to condition the biosensors for either CV or CA methods (Cond.V1 and Cond.V2 in Fig. 1). In this way, when one WE is connected to the measurement circuit, the other WEs can go through the conditioning phase to be ready for measurement afterwards. When there is no request to do a measurement, WE can be connected to one of the below options: 1) Ground; 2) CE; 3) A fixed voltage for CA conditioning; 4) A ramp voltage for CV conditioning;

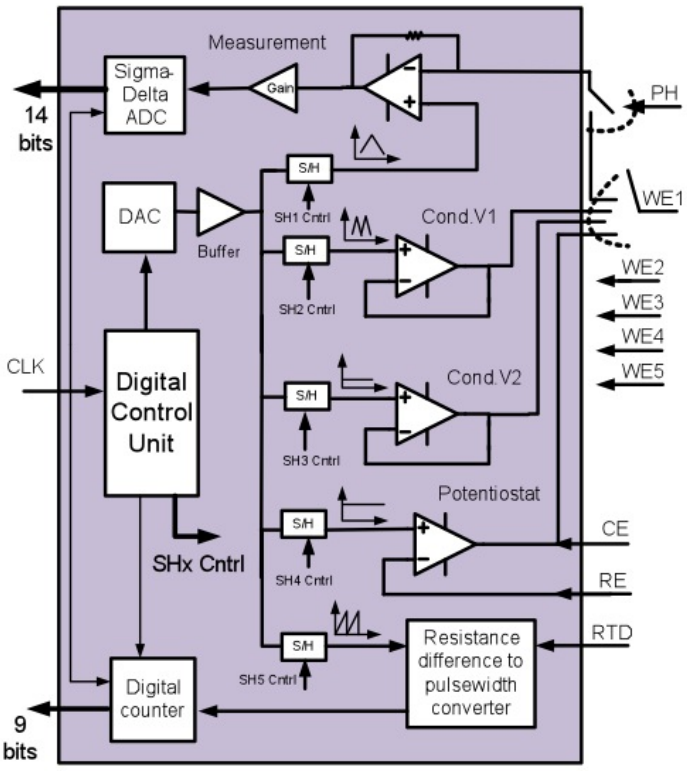

Fig. 1. Architecture of the IC to control and readout multi-target biosensor.

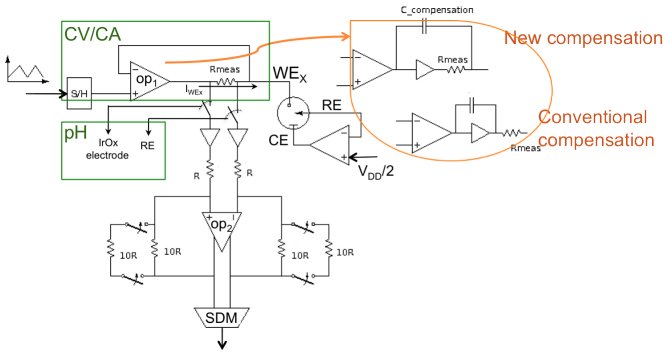

Fig. 2. The schematic view of the circuit for CV, CA and pH readout. A fixed or triangular waveform is applied to the WEx and the resulting current is measured through R_{meas} and amplified before going through the ADC.

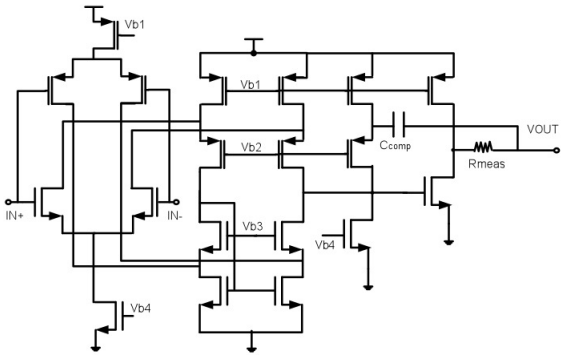

Fig. 3. The schematic view of the compensated opamp for CV and CA readout (OP_1 in Fig. 2). It remains stable for $C_{load} \geq 500\ pF$.

5) or no connection. Through this, it is possible to study the interference of an adjacent WE with the measured data.

To reduce the power consumption and the area of the IC, a DDS is shared among different circuits to generate 5 different voltage profiles: 1) Triangular waveform for CV; 2) Fixed voltage for CA; 3) Fixed or 4) triangular voltage for conditioning; 5) Sawtooth waveform for the temperature sensing circuit. The *sample and hold* (SH) circuits are used to enable DDS sharing when different voltage profiles are needed at the same time. The required control signals to refresh SH's (signals SHx Cntrl in Fig. 1) are generated on-chip through the digital control unit.

Three major blocks are described in the following subsections: i) Unified circuit for pH, CV and CA readout; ii) Sigma delta ADC; iii) Resistance difference to pulsewidth converter.

A. Unified circuit for CV, CA, and pH readout

In this work, an innovative circuit for biosensor readout is designed that is capable of CV and CA control and readout as well as pH readout. The schematic of the circuit is shown in Fig. 2. For CV measurement a fixed voltage (e.g. $V_{DD}/2$ in Fig. 2) is applied to the RE through the potentiostat while a triangular waveform is applied to the WE of interest.

The resulting current (I_{WEx} in Fig. 5), which is the signal of the biosensor and carries the information about the concentration and type of the target molecules, flows into the resistance R_{meas}. In the most common scenario the triangular waveform sweeps the voltage from $0.4\ V$ to $1.4\ V$ with a slope of $20\ mV/sec$. Note that when the voltage at the WE is at its maximum, the current flows out of OP_1. This results in a voltage that is higher than $1.4\ V$ at the output of OP_1. To insure linear measurement of the sensor current, the value of the resistance is chosen such that the maximum voltage drop across it is less than $300\ mV$.

A new method has been used to compensate OP_1 for a wide range of load capacitors. The conventional compensation method for a two stage amplifier is to connect a capacitor between the outputs of the two stages. According to [11] some modifications can be applied to the connection point of the capacitor to the first stage to remove the right-plane zero. In this circuit, we changed the connection point of the compensation capacitor from the output of the second stage of the amplifier to WE_x. Therefore, the feedback loop encloses the resistance R_{meas}. Simulations show that the new phase margin is more than $45°$ for any load capacitor more than $500\ pF$, while without any compensation it is $200\ nF$, and with the conventional method it is $30\ nF$, for the same compensation capacitor value. The schematic view of the readout amplifier with the new compensation method is shown in Fig. 3. The bias circuit is not shown for simplicity.

The voltage across R_{meas} is buffered using two full-swing amplifiers. The buffered differential voltage is amplified using the differential amplifier OP_2. OP_2 is a folded cascade amplifier with common mode feedback. The gain and bandwidth of OP_2 are $52\ dB$ and $8.5\ kHz$, respectively. The output of OP_2 goes through a sigma-delta ADC to be digitized. The OP_2 acts as the anti-aliasing filter for the ADC. Simulations show that the error in current measurement due to the compensation

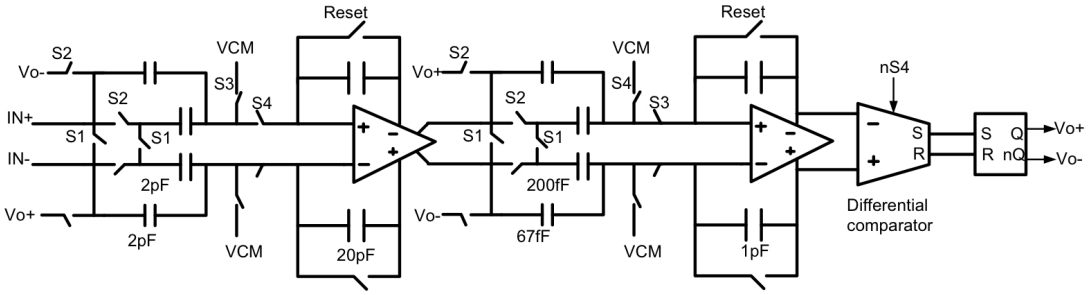

Fig. 4. The schematic view of the second order sigma-delta modulator. The capacitors are chosen such that the modulator gives 14-bit accuracy.

capacitor, and the input current of the buffers is negligible in low frequencies (i.e. less than $10\ Hz$), introducing no error in the measurement result.

pH measurement is realized by disconnecting the buffers from the R_{meas} and connecting one of them to RE and the other one to an IrOx coated electrode that has been designed for pH sensing. The voltage difference between this electrode and RE changes linearly with the pH of the sensor wet interface [12].

B. Sigma-delta ADC

A second order sigma-delta modulator is designed to digitize the measured data. The capacitors in the first and second integrator are chosen such that the modulator gives 14-bit accuracy for a signal bandwidth of $1\ kHz$ with a clock frequency of $512\ kHz$. The amplifiers are realized with a folded-cascade stage. The switch-capacitor common mode feedback method from [13] is used to set the output common mode voltage of the amplifiers at $V_{DD}/2$. The schematic view of the sigma-delta modulator is shown in Fig.4. S_1, S_2, S_3, and S_4 are non-overlapping clock signals, generated by an on-chip clock generator block, to control the switches.

The common mode voltage of the differential amplifiers as well as the common mode voltage of the integrators (VCM in Fig. 4) is provided on-chip by a bandgap reference circuit which is designed similar to [14] to generate $0.9\ V$. Simulation results in different corners and temperatures from $30°C$ to $80°C$ show less than $20\ \mu V$ variation in the generated voltage.

C. Temperature measurement

The circuit for temperature measurement is based on comparison of a platinum *resistance temperature detection* (RTD) with an on-chip reference resistor.

The schematic of the circuit is shown in Fig. 5. The threshold voltage of the two comparators are set to $R_{RTD} \times I_{ref1}$ and $R_{ref} \times I_{ref2}$. I_{ref1} and I_{ref2} are mirrored currents of a reference current, I_{ref}, and are theoretically equal. The current source is designed using an N-MOSFET biased in its *zero temperature coefficient* (ZTC) bias point. The gate-source voltage of the N-MOSFET in its ZTC is provided by the bandgap reference circuit. A sawtooth waveform is applied to the other terminal of the comparators. The difference in the threshold voltage of the comparators is proportional to the difference of R_{RTD} and R_{ref}. Any difference in the threshold voltages translates into different transition times in the output

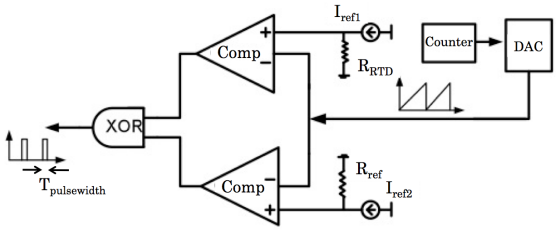

Fig. 5. The schematic view of the temperature measurement circuit using a Platinum RTD. The circuit converts the resistance difference into pulse width.

of the comparator. The XOR gate detects the time difference between transitions that can be calculated by:

$$T_{pulsewidth} = \frac{T_{sawtooth}}{\frac{V_{DD}}{2^{NOB}}} \times I_{ref} \times (R_{RTD} - R_{ref}) \qquad (1)$$

Where $T_{sawtooth}$ is the period of the sawtooth waveform and NOB is the DAC number of bits which is 9 in our design. The pulse-width is measured on-chip using a digital counter that works with a frequency of $\frac{2^{NOB}}{T_{sawtooth}}$.

III. Simulation results

A. Unified circuit for CV, CA, and pH readout

Simulations on the CV and CA readout are done using the RC equivalent model of the biosensor [4], [7]. The summary of the circuit specifications is presented in table I. According to [12], the open circuit voltage at the output of the pH sensor is from $-30\ mV$ to $+120\ mV$ for pH from 5 to 8. Assuming an ideally linear pH sensor, our circuit is able to detect pH from 1.5 to 13.5 with 0.0003 resolution.

B. sigma-delta modulator

The output *power spectral density* (PSD) of the sigma-delta modulator is simulated after extracting the parasitic resistances and capacitances from the layout and is shown in Fig.7. The effective number of bits in the signal bandwidth of $1\ kHz$ is 13.5 bits for a differential input voltage of $800\ mV$.

C. Temperature measurement

The output of the digital counter versus the temperature difference between the R_{RTD} and R_{ref} is presented in Fig.8

TABLE I
SIMULATION RESULTS ON THE CIRCUIT FOR CV, CA, AND PH READOUT

Readout	Linear range (5%)	Resolution (@ 1 Hz)
CV, CA	$\pm 2.3\ uA$	125 pA (input referred current noise)
pH	$\pm 300\ mV$	16 μV (input referred voltage noise)

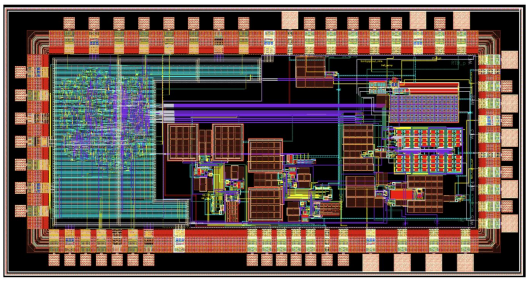

Fig. 6. Layout view of the interface electronic IC in $0.18\ \mu m$ technology

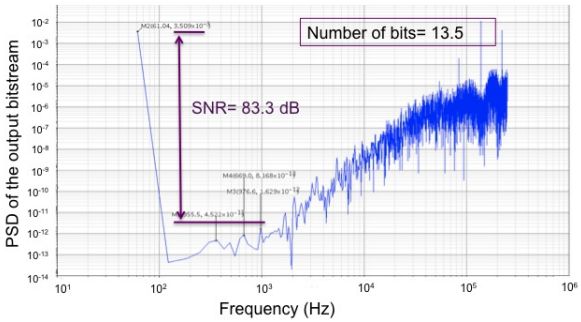

Fig. 7. PSD of the sigma-delta modulator output (post layout simulation).

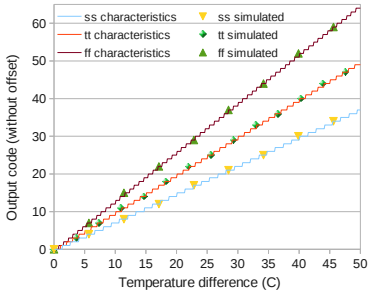

Fig. 8. Characteristics of the temperature sensor in different corners.

TABLE II
POWER CONSUMPTION THE INTERFACE ELECTRONICS

Block name	Power consumption (μW)
Sigma-delta modulator	350
common circuit for CV,CA and pH	198
Added circuit for CV/CA	30
Potentiostat	36
Conditioning circuits	3
DAC+buffer	3 + 28
Temperature sensor	12
Bandgap reference + Buffer	3 + 48
Total	**711**

for different technology corners. While the linearity of the measurement is held in different corners, the accuracy changes. The resulted resolution in fast, typical and slow corners are $0.74°C$, $0.96°C$, and $1.28°C$ respectively.

IV. CONCLUSIONS

A configurable IC for control/readout different molecular sensors through five sensing sites is designed in $0.18\ \mu m$ technology and presented. A waveform generator is designed to provide different voltage profiles to control or condition the sensors for both CV and CA measurements. The bidirectional current of less than $2.3\ \mu A$ can be measured and digitized with 13.5 bits resolution through a highly stable readout amplifier and a sigma-delta ADC. The pH and temperature can also be measured with resolution of 0.0003 and better than $1.28°C$, respectively. Thanks to sharing some of the main blocks among different circuits, the power consumption of the IC is limited to $711\ \mu W$ from $1.8\ V$ supply voltage, and its area is $1.5\ mm \times 3.2\ mm$, making it suitable for implantable applications [15].

V. ACKNOWLEDGEMENT

The research has been funded by the project i-IronIC that is financed with a grant from the Swiss Nano-Tera.ch initiative and evaluated by the Swiss National Science Foundation.

REFERENCES

[1] A. J. Bard and L. R. Faulkner, *Electrochemical methods: fundamentals and applications*. Willey, 1980.

[2] G. De Micheli, S. Ghoreishizadeh, C. Boero, F. Valgimigli, and S. Carrara, "An integrated platform for advanced diagnostics," in *Design, Automation Test in Europe Conference Exhibition*, 2011, pp. 1–6.

[3] C. Boero, J. Olivo, G. De Micheli, and S. Carrara, "New approaches for carbon nanotubes-based biosensors and their application to cell culture monitoring," *Biomedical Circuits and Systems, IEEE Trans. on*, vol. 6, no. 5, pp. 479–485, 2012.

[4] M. Ahmadi and G. Jullien, "Current-mirror-based potentiostats for three-electrode amperometric electrochemical sensors," *Circuits and Systems I: Regular Papers, IEEE Trans. on*, vol. 56, no. 7, pp. 1339 –1348, 2009.

[5] M. Haider, S. Islam, S. Mostafa, M. Zhang, and T. Oh, "Low-power low-voltage current readout circuit for inductively powered implant system," *Biomedical Circuits and Systems, IEEE Trans. on*, vol. 4, no. 4, pp. 205 –213, 2010.

[6] Y.-T. Liao, H. Yao, A. Lingley, B. Parviz, and B. Otis, "A 3- CMOS glucose sensor for wireless contact-lens tear glucose monitoring," *Solid-State Circuits, IEEE Journal of*, vol. 47, no. 1, pp. 335 –344, 2012.

[7] P. Levine, P. Gong, R. Levicky, and K. L. Shepard, "Active CMOS sensor array for electrochemical biomolecular detection," *Solid-State Circuits, IEEE Journal of*, vol. 43, no. 8, pp. 1859–1871, 2008.

[8] L. Li, X. Liu, W. Qureshi, and A. Mason, "CMOS amperometric instrumentation and packaging for biosensor array applications," *Biomedical Circuits and Systems, IEEE Trans. on*, vol. 5, no. 5, pp. 439–448, 2011.

[9] K. B. Koller and F. M. Hawkridge, "The effects of temperature and electrolyte at acidic and alkaline ph on the electron transfer reactions of cytochrome c at in2o3 electrodes," *Journal of Electroanalytical Chemistry and Interfacial Electrochemistry*, vol. 239, no. 12, pp. 291 – 306, 1988.

[10] S. Ghoreishizadeh, C. Baj-Rossi, S. Carrara, and G. De Micheli, "Nano-sensor and circuit design for anti-cancer drug detection," in *Life Science Systems and Applications Workshop (LISSA)*, 2011, pp. 28–33.

[11] B. Ahuja, "An improved frequency compensation technique for CMOS operational amplifiers," *Solid-State Circuits, IEEE Journal of*, vol. 18, no. 6, pp. 629–633, 1983.

[12] A. Cavallini, C. Baj-Rossi, S. Ghoreishizadeh, G. De Micheli, and S. Carrara, "Design, fabrication, and test of a sensor array for perspective biosensing in chronic pathologies," in *Biomedical Circuits and Systems Conference (BioCAS), 2012 IEEE*, Nov., pp. 124–127.

[13] O. Choksi and L. Carley, "Analysis of switched-capacitor common-mode feedback circuit," *Circuits and Systems II: Analog and Digital Signal Processing, IEEE Trans. on*, vol. 50, no. 12, pp. 906–917, 2003.

[14] H. Banba, H. Shiga, A. Umezawa, T. Miyaba, T. Tanzawa, S. Atsumi, and K. Sakui, "A CMOS bandgap reference circuit with sub-1-v operation," *Solid-State Circuits, IEEE Journal of*, vol. 34, no. 5, pp. 670–674, 1999.

[15] S. Carrara, S. Ghoreishizadeh, J. Olivo, I. Taurino, C. Baj-Rossi, A. Cavallini, M. Op de Beeck, C. Dehollain, W. Burleson, F. G. Moussy, A. Guiseppi-Elie, and G. De Micheli, "Fully integrated biochip platforms for advanced healthcare," *Sensors*, vol. 12, no. 8, pp. 11 013–11 060, 2012.